ISSN 1063-7761, Journal of Experimental and Theoretical Physics, 2013, Vol. 116, No. 5, pp. 817–822. © Pleiades Publishing, Inc., 2013.
Original Russian Text © V.V. Val'kov, A.O. Zlotnikov, 2013, published in Zhurnal Eksperimental'noi i Teoreticheskoi Fiziki, 2013, Vol. 143, No. 5, pp. 941–947.

ORDER, DISORDER, AND PHASE TRANSITION IN CONDENSED SYSTEM

Anomalous Properties and Coexistence of Antiferromagnetism and Superconductivity near a Quantum Critical Point in Rare-Earth Intermetallides[1]

V. V. Val'kov[a,b,*] and A. O. Zlotnikov[a]

[a] *Kirensky Institute of Physics, Siberian Branch, Russian Academy of Sciences, Krasnoyarsk, 660036 Russia*

* *e-mail: vvv@iph.krasn.ru*

[b] *Siberian State Aerospace University, Krasnoyarsk, 660014 Russia*

Received July 2, 2012

Abstract—Mechanisms of the appearance of anomalous properties experimentally observed at the transition through the quantum critical point in rare-earth intermetallides have been studied. Quantum phase transitions are induced by the external pressure and are manifested as the destruction of the long-range antiferromagnetic order at zero temperature. The suppression of the long-range order is accompanied by an increase in the area of the Fermi surface, and the effective electron mass is strongly renormalized near the quantum critical point. It has been shown that such a renormalization is due to the reconstruction of the quasiparticle band, which is responsible for the formation of heavy fermions. It has been established that these features hold when the coexistence phase of antiferromagnetism and superconductivity is implemented near the quantum critical point.

DOI: 10.1134/S1063776113050129

1. The destruction of the long-range order at the quantum phase transition is caused by an increase in quantum fluctuations whose intensity is governed by a control parameter (e.g., pressure) [1, 2]. The application of hydrostatic pressure in cerium intermetallides at temperatures below the Néel temperature suppresses the long-range antiferromagnetic order, leading to its sharp destruction at the quantum phase transition. In this case, a transition to a superconducting state is observed near the quantum critical point.

The $CeRhIn_5$ compound is of particular interest in recent years because the coexistence phase of superconductivity and antiferromagnetism, which is homogeneous at the microscopic scale, is implemented in it [3]. The role of cerium ions and itinerant p states of indium atoms is significant in the formation of the electronic structure of this compound [4]. It was shown that hybridization mixing is implemented between $4f$ Ce states and p In states [5]. These facts underlie the assumption that the periodic Anderson model can be used for the qualitative description of features of the low-energy spectrum of Fermi excitations in $CeRhIn_5$. In this description, it is accepted that the subsystem of $4f$ electrons is responsible for the formation of both the antiferromagnetic order and Cooper instability.

The first approach to the problem of quantum critical points is based on the generalization of the fluctuation theory of phase transitions to the case of zero temperature [6]. It was shown in [7] that quantum fluctuations can make significant corrections to the thermodynamic properties of a itinerant electron system. To determine the role of localized electrons in the critical region, the concept of the local quantum critical point was proposed more recently [8]. The transition from the paramagnetic region through such a critical point is accompanied by the appearance of the long-range antiferromagnetic order and by the violation of the Kondo regime induced owing to the s–$d(f)$ coupling between itinerant and localized electrons.

The transition through the quantum critical point in some heavy-fermion systems is accompanied by the appearance of anomalous properties. This concerns primarily the effective electron mass whose dependence on the control parameter exhibits divergence in the region of the quantum phase transition. Moreover, the Fermi surface grows [9]. These effects were detected when analyzing the pressure dependence of the frequency of de Haas–van Alphen oscillations in $CeRhIn_5$ [10]. An additional feature is associated with the implementation of a non-Fermi liquid regime [11]. In particular, the temperature dependence of the electrical resistivity near the quantum critical point in the $CeRhIn_5$ compound becomes almost linear [12]. Such a dependence is implemented, e.g., in the two-band model [13].

[1] The article is based on a preliminary report delivered at the 36th Conference on Low-Temperature Physics (St. Petersburg, July 2–6, 2012).

Deviations from the Fermi-liquid behavior are not necessarily due to the closeness to the quantum critical point. In particular, the phenomenological two-liquid model [14] implies that the thermodynamic characteristics below the coherence temperature are determined by two contributions. The first contribution comes from the appearance of the heavy-fermion coherent state caused by the hybridization between localized and conduction electrons. The second contribution comes from isolated Kondo impurities remaining in the system on which spin–fluctuation scattering occurs.

Several scenarios of the anomalous behavior of the effective mass and cross section of the Fermi surface are under discussion now. One of them is associated with the violation of the Kondo regime at the local quantum critical point [9]. According to this scenario, when the Kondo regime is broken, the Fermi surface is formed only by itinerant electrons. For this reason, the area of the Fermi surface decreases. Another mechanism is attributed to the presence of strong valence fluctuations [15].

The possibility of implementing the coexistence phase of antiferromagnetism and superconductivity in heavy-fermion intermetallides is analyzed in this work within the extended periodic Anderson model and it is shown that the effective electron mass anomalously increases near the quantum critical point. In this case, the quantum phase transition is accompanied by a sharp change in the Fermi surface.

2. To describe the anomalous behavior of quasiparticle characteristics observed near the implementation boundary of the antiferromagnetic state in heavy-fermion compounds, we consider the Anderson model in the atomic representation [16, 17]. In the Hamiltonian of such a system, we separate the effective interaction responsible for the formation of the long-range antiferromagnetic order:

$$\hat{H}_{\text{eff}} = \hat{H}_{\text{PAM}} + \hat{H}_{\text{exch}}. \tag{1}$$

The Hamiltonian of the periodic Anderson model $\hat{H}_{\text{PAM}}$ in the strong electron correlation regime is given by the usual expression

$$\begin{aligned}\hat{H}_{\text{PAM}} = &\sum_{m\sigma}(\varepsilon_0 - \mu)c^{\dagger}_{m\sigma}c_{m\sigma} + \sum_{ml\sigma}t_{ml}c^{\dagger}_{m\sigma}c_{l\sigma}\\ &+ \sum_{m\sigma}(E_0 - \mu)X^{\sigma\sigma}_m\\ &+ \sum_{ml\sigma}[V_{ml}c^{\dagger}_{m\sigma}X^{0\sigma}_l + V^{*}_{ml}X^{\sigma 0}_l c_{m\sigma}].\end{aligned} \tag{2}$$

Here, $c_{m\sigma}$ are the Fermi operators in the Wannier representation, ε_0 is the one-site energy of electron states, t_{ml} is the hopping integral, E_0 is the bare energy of localized states, μ is the chemical potential, and $X^{0\sigma}_l$ are the quasi-Fermi Hubbard operators. The intensity of the hybridization of wavefunctions of itinerant and localized electrons is determined by the matrix elements V_{ml}. The interaction between localized electrons is described by the operator

$$\hat{H}_{\text{exch}} = \frac{1}{4}\sum_{ml\sigma}J_{ml}(X^{\sigma\bar{\sigma}}_m X^{\bar{\sigma}\sigma}_l - X^{\sigma\sigma}_m X^{\bar{\sigma}\bar{\sigma}}_l). \tag{3}$$

Such an interaction appears in the periodic Anderson model after the inclusion of high-energy hybridization processes [18].

3. To derive self-consistency equations, we use the method of irreducible two-time temperature Green's functions [19] and the Zwanzig–Mori projection formalism. To describe the antiferromagnetic phase, it is sufficient to take into account a two-sublattice set of basis operators (sites f and g belong to the F and G sublattices, respectively):

$$(X^{0\sigma}_f, Y^{0\sigma}_g, a_{f\sigma}, b_{g\sigma}). \tag{4}$$

Deriving the equations for the Green's functions using the indicated method and solving the resulting system of equations, we obtain the explicit expressions for the desired Green's functions:

$$\begin{aligned}\langle\langle X_{p\sigma}|X^{\dagger}_{p\sigma}\rangle\rangle_{\omega} &= \frac{\alpha_{\sigma}S_{p\sigma}(\omega)}{d_4(p,\omega)},\\ \langle\langle a_{p\sigma}|a^{\dagger}_{p\sigma}\rangle\rangle_{\omega} &= \frac{C_{p\sigma}(\omega)}{d_4(p,\omega)}\end{aligned} \tag{5}$$

for the electrons in the localized subsystem and itinerant electrons, respectively. In Eqs. (5),

$$\begin{aligned}S_{p\sigma}(\omega) &= (\omega - E_{\bar{\sigma}})[(\omega - \xi_p)^2 - \Gamma^2_p]\\ &- \alpha_{\bar{\sigma}}(\omega - \xi_p)(V^2_p + W^2_p) - 2\alpha_{\bar{\sigma}}\Gamma_p V_p W_p,\\ C_{p\sigma}(\omega) &= (\omega - E_{\sigma})(\omega - E_{\bar{\sigma}})(\omega - \xi_p)\\ &- \alpha_{\bar{\sigma}}(\omega - E_{\sigma})V^2_p - \alpha_{\sigma}(\omega - E_{\bar{\sigma}})W^2_p.\end{aligned} \tag{6}$$

The dispersion equation determining the energy spectrum of the system is obtained from the condition that the denominator of the resulting Green's functions is zero:

$$\begin{aligned}d_4(p,\omega) &= (\omega - E_{\sigma})(\omega - E_{\bar{\sigma}})[(\omega - \xi_p)^2 - \Gamma^2_p]\\ &+ \alpha_{\sigma}\alpha_{\bar{\sigma}}(V^2_p - W^2_p)^2 - [\alpha_{\sigma}(\omega - E_{\bar{\sigma}}) + \alpha_{\bar{\sigma}}(\omega - E_{\sigma})]\\ &\times [(\omega - \xi_p)(V^2_p + W^2_p) + 2\Gamma_p V_p W_p] = 0.\end{aligned} \tag{7}$$

The physical meaning of the introduced notation is as follows. The renormalized expression for the energy of the localized level, $E_{\sigma} = E_0 - \mu - J(n_L + 2\eta_{\sigma}R)$, includes a correction associated with the mean-field effect of the exchange interaction (contribution of about $-Jn_L$) and a contribution of about $-2\eta_{\sigma}JR$ ($\eta_{\sigma} = \pm 1$, $\sigma = \uparrow, \downarrow$), which leads to the lift of the degeneracy of this level in the projection of the spin. The quantity $\xi_p = \varepsilon_0 + t_p - \mu$ is the part of the kinetic energy of itinerant electrons that is measured from the

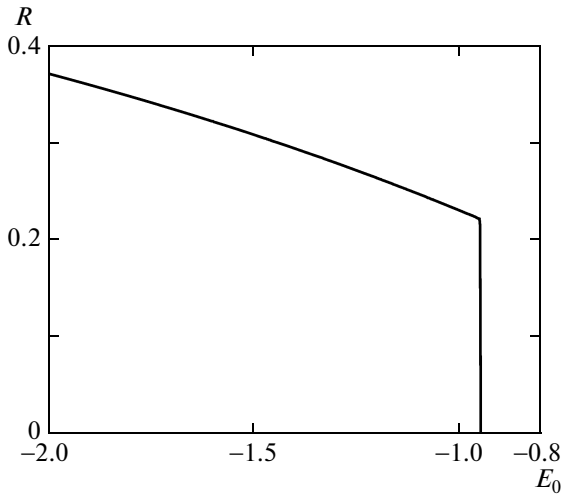

Fig. 1. Magnetization of the antiferromagnetic sublattice R versus the energy of localized states E_0 at the electron concentration $n_e = 1.1$ for the model parameters $V_0 = 0.6$ and $J = 0.2$.

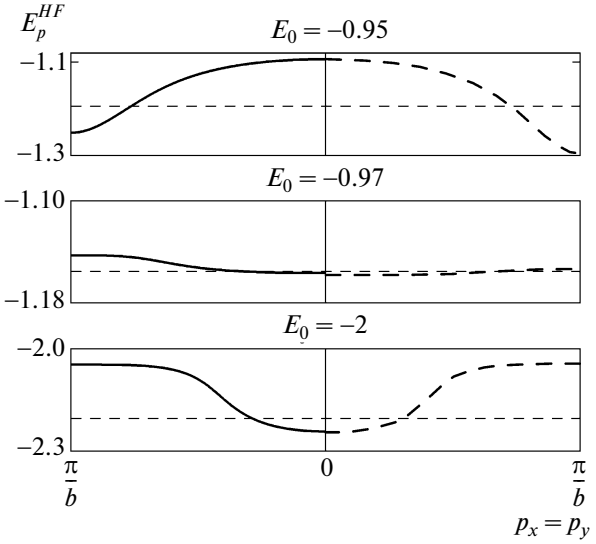

Fig. 2. Modification of the quasiparticle band corresponding to heavy fermions with increasing energy E_0 and at the transition from (two lower panels) the antiferromagnetic phase to (upper panel) the paramagnetic phase. The thin dashed line indicates the chemical potential. The calculation parameters are the same as in Fig. 1.

chemical potential and is associated with intrasublattice hopping. The functions t_p, Γ_p, V_p, and W_p are determined in terms of the Fourier transforms of $t_{ff'}$, t_{fg}, $V_{ff'}$, and V_{fg}.

The average number of localized electrons $n_L = \sum_\sigma \langle X_f^{\sigma\sigma} \rangle$ and the magnetization of the antiferromagnetic sublattice $R = \sum_\sigma \eta_\sigma \langle X_f^{\sigma\sigma}/2 \rangle$ are unknown and characterize the ground state of the system. The Hubbard renormalization for the antiferromagnetic phase is represented in terms of these parameters as $\alpha_\sigma = \alpha + \eta_\sigma R$ (where $\alpha = 1 - n_L/2$ is the standard renormalization in the paramagnetic phase). To calculate n_L and R, we use the self-consistency procedure in the equation obtained using the spectral theorem,

$$\langle X_f^{\sigma\sigma} \rangle = \frac{1}{N} \sum_{kj} \alpha_\sigma \frac{S_{k\sigma}(E_{jk}) f(E_{jk}/T)}{\prod_{i \neq j} (E_{jk} - E_{ik})}, \qquad (8)$$

where $f(x) = 1/(e^x + 1)$ is the Fermi–Dirac function and subscripts j and i vary from 1 to 4, which correspond to the contribution from four branches of the energy spectrum E_{jk} in the antiferromagnetic phase.

Figure 1 shows the dependence of the magnetization R on the bare energy of the localized level at zero temperature. The energies are measured in units of the hopping parameter of itinerant electrons between nearest neighbors $|t_1|$. It can be seen that an increase in the energy E_0 is accompanied by a decrease in the magnetization. When E_0 reaches the critical value (quantum critical point), the magnetization of the system vanishes (the long-range antiferromagnetic order disappears). It is noteworthy that the suppression of the antiferromagnetic order in this case is determined by the control parameter E_0. A change in this parameter is usually associated with the external pressure.

4. The shape of the Fermi surface and the effective mass are determined by solving dispersion equation (7). To simplify the calculations, we consider only the energy range in which a narrow hybridized band associated with the heavy-fermion band is located. For this energy band, an approximate analytical expression [20] determining the quasimomentum dependence of the heavy-fermion band in the antiferromagnetic phase can be obtained in the form

$$E_p^{\mathrm{HF}} = -(1 - \alpha\gamma_p)|E_J| - \frac{\tau_p}{\Gamma_p^2 - E_J^2}, \qquad (9)$$

where

$$\tau_p = \sqrt{(\alpha^2 - R^2)\Gamma_p^2 V_p^4 + (2J(\Gamma_p^2 - E_J^2) - |E_J| V_p^2)^2 R^2}.$$

It is accepted that the shifted localized level $E_J = E_0 - Jn_L$ intersects the lower antiferromagnetic subband of itinerant electrons ($E_J < 0$). In derivation, we used the nearest neighbor approximation for electron hopping and take into account only one-site and intrasublattice hybridization processes.

Figure 2 shows the dispersion dependences of the heavy-fermion band along the principal direction of the magnetic Brillouin zone for various energies E_0. The lower two panels correspond to the spectrum of heavy fermions in the antiferromagnetic state and the upper panel corresponds to the paramagnetic state. The

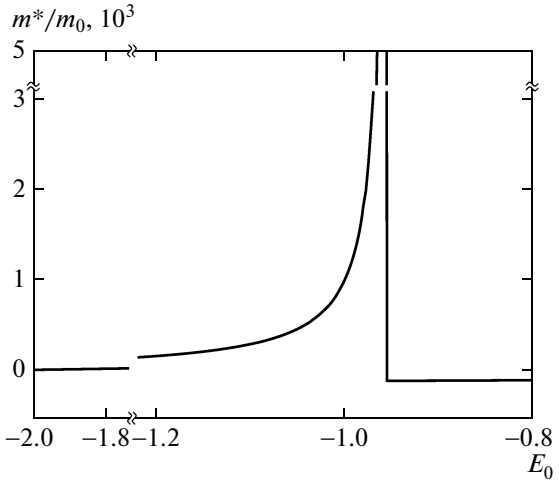

Fig. 3. Anomalous increase in the effective electron mass at the quantum phase transition from the antiferromagnetic phase to the paramagnetic phase.

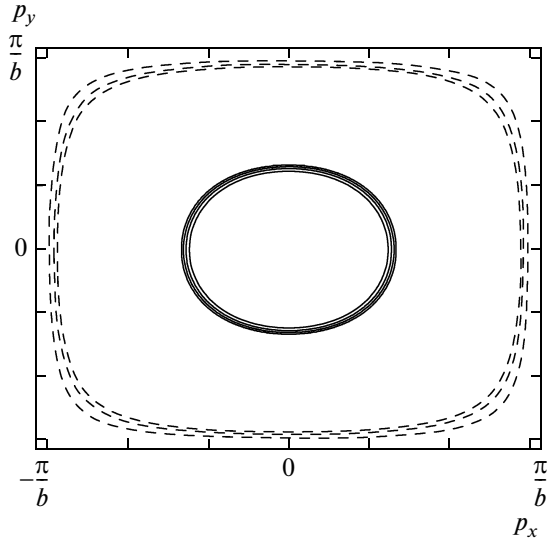

Fig. 4. Fermi surfaces in (solid lines) the antiferromagnetic phase for the energy $E_0 = -2$, -1.5, -1.2, and -0.97 and in (dashed lines) the paramagnetic phase for the energy $E_0 = -0.95$, -0.8, and -0.5. The lowest energy corresponds to the smallest Fermi surface.

dashed lines are obtained by approximate formula (9) and the solid lines are calculated from Eq. (7). It can be seen that an increase in the energy E_0, which leads to a decrease in the magnetization according to Fig. 1, is accompanied by the narrowing of the heavy-fermion band and the structure of this band changes qualitatively at the transition to the paramagnetic phase.

A decrease in the width of the heavy-fermion band leads to an increase in their effective mass. The effective electron mass divided by the bare mass of the itinerant electron $m_0 = \hbar^2/|t_1|\,b$ (b is the lattice parameter) is estimated by the expression

$$\frac{m^*}{m_0} = \frac{(\Gamma_0^2 - E_J^2)^2\tau_0}{|\Gamma_0|V_0^2}\{2\alpha|E_J|\tau_0 - [(\alpha^2 - R^2)\Gamma_0^2 + (\alpha^2 + R^2)E_J^2]V_0^2 + 4JR^2|E_J|(\Gamma_0^2 - E_J^2)\}^{-1}.$$

Figure 3 shows the effective electron mass as a function of the energy E_0. It can be seen that the dependence of the mass on the control parameter is anomalous near the quantum critical point ($E_0 \approx -0.95$). The effective mass becomes negative above the antiferromagnetic–paramagnetic transition. This means that the type of charge carriers changes at the quantum critical point.

The condition determining the strong renormalization of the mass has the form

$$E_0 = -\frac{V_0^2}{4J}\frac{\alpha - R}{R} + Jn_L. \quad (10)$$

It is taken into account that the density of localized electrons and the magnetization depend on the energy E_0.

According to Eq. (10), the divergence of the mass of heavy fermions occurs near the quantum critical point and correlates with the modification of the heavy-fermion band at the quantum phase transition (Fig. 2). As a parameter describing this modification, we use the width of the heavy-fermion band for the principal direction given by the expression

$$W_{\mathrm{HF}} = -\frac{\alpha V_0^2\Gamma_0^2}{(\Gamma_0^2 - E_J^2)|E_J|} + \frac{1}{|E_J|}(2J|E_J| + V_0^2)R + \frac{\tau_0}{\Gamma_0^2 - E_J^2}. \quad (11)$$

It is easy to verify that the width of the band decreases with a decrease in the magnetization and an increase in the energy E_0. The quasimomentum dependence of the energy spectrum in the paramagnetic region is inverted as compared to the dependence of the spectrum in the antiferromagnetic phase. Consequently, an extremely narrow band with a large effective mass can appear as the width of the band in the antiferromagnetic phase decreases. It can be shown that Eq. (10) at which the effective electron mass diverges is a solution of the equation $W_{\mathrm{HF}} = 0$. Thus, the divergence of the electron mass is due to the strong reduction of the heavy-fermion band. The appearance of the weakly disperse narrow band in turn indicates the closeness of the quantum phase transition.

The broadening of the Fermi surface at the transition through the quantum critical point is illustrated in Fig. 4. The solid and dashed lines show the Fermi surfaces for various energies E_0 in the antiferromagnetic and paramagnetic phases, respectively. It can be seen that the size of the Fermi surface in the antiferromagnetic phase is almost independent of the energy E_0 and several curves merge to one. However, the Fermi sur-

face expands strongly at the transition through the antiferromagnetic–paramagnetic boundary. A further increase in the energy E_0 in the paramagnetic phase does not lead to such a strong increase in the Fermi momentum. This behavior is caused by a change in the type of charge carriers at the quantum phase transition point. Thus, the transition from the effectively electron Fermi surfaces to hole Fermi surfaces occurs at the quantum critical point. Therefore, significant anomalies in the Hall effect will be observed at the quantum phase transition.

5. Interaction (3) in the proposed model can induce Cooper instability. The experimental data for $CeRhIn_5$ indicate that the superconducting phase at pressures above the critical value has *d*-wave symmetry. In the coexistence phase of superconductivity and antiferromagnetism, the symmetry of the order parameter is not determined; it is assumingly *d*-wave symmetry, but with additional nodal points on the Fermi surface [21]. It is significant that the consideration of superconducting *d*-wave pairing against the background of the antiferromagnetic ordering is in qualitative agreement with the phase diagram of $CeRhIn_5$.

To analyze the coexistence phase of superconductivity and antiferromagnetism, it is necessary to use the basis set of operators that makes it possible to take into account both anomalous averages and anomalous Green's functions. For this reason, we use the extended basis

$$(X_f^{0\sigma}, Y_g^{0\sigma}, a_{f\sigma}, b_{g\sigma}, X_f^{\bar{\sigma}0}, Y_g^{\bar{\sigma}0}, a_{f\bar{\sigma}}^{\dagger}, b_{g\bar{\sigma}}^{\dagger}) \quad (12)$$

instead of basis (4). Deriving the equations for normal and anomalous Green's functions and projecting on the set of irreducible Green's functions corresponding to basis (12), we obtain a closed system of equations. This system is solved taking into account experimental information that the superconducting order parameter assumingly has *d*-wave symmetry. This order parameter is given by the expression

$$\Delta_p^d = 2\Delta_0^d \sin\left(\frac{p_x b}{2}\right)\sin\left(\frac{p_y b}{2}\right). \quad (13)$$

Since the amplitude Δ_0^d in the coexistence phase of superconductivity and antiferromagnetism is small, the energy spectrum of heavy fermions is modified insignificantly as compared to the spectrum given by Eq. (9). For this reason, the quasiparticle characteristics of fermions in this phase will be well described by the expressions presented in the preceding section.

The self-consistency equations for the superconducting phase allow solutions for which the symmetry of the order parameter can differ from *d*-wave symmetry. The analysis shows that the superconducting phase with *d*-wave symmetry without the antiferromagnetic order has a higher critical temperature and, therefore, a higher condensation energy. This corresponds to the experimental situation. According to the calculations, the appearance of the antiferromagnetic order can lead to a change in the results of the competition between superconducting phases with the *d*-wave and *s*-wave symmetries of the order parameter. However, at a small antiferromagnetic order parameter, its effect will be small and the *d*-wave phase will be preferable. The complete analysis of this problem is beyond the scope of this work and will be reported elsewhere.

6. To conclude, it is noteworthy that the inclusion of the exchange interaction in the subsystem of localized electrons leads to the possibility of implementing the antiferromagnetic phase, superconducting phase, and microscopically homogeneous coexistence phase of superconductivity and antiferromagnetism. The regime has been revealed at which the effective electron mass increases anomalously and the Fermi surface expands similar to a behavior in a number of rare-earth intermetallic systems with an increase in the pressure. It has been shown that the divergence of the mass of heavy fermions occurs in the antiferromagnetic phase immediately near the quantum phase transition point to the paramagnetic phase. The divergence of the mass is accompanied by the formation of the weakly disperse band of heavy fermions. This behavior of *f* electrons occurs only near the quantum critical point. In the antiferromagnetic phase region far from the quantum phase transition, an increase in the magnetization of the antiferromagnetic sublattice leads to a decrease in the effective electron mass.

ACKNOWLEDGMENTS

We are grateful to K. Kikoin and D. Dzebisashvili for useful remarks. This work was supported by the Presidium of the Russian Academy of Sciences (program "Quantum Mesoscopic and Disordered Structures"), the Russian Foundation for Basic Research (project nos. 10-02-00251, 11-02-98007-Siberia, and 12-02-31130), (project 14.132.21.1410), and the grant of the President of the Russian Federation (project MK-526.2013.2).

REFERENCES

1. S. M. Stishov, Phys.—Usp. **47** (8), 789 (2004).
2. V. F. Gantmakher and V. T. Dolgopolov, Phys.—Usp. **51** (1), 3 (2008).
3. T. Mito, S. Kawasaki, Y. Kawasaki, G.-Q. Zheng, Y. Kitaoka, D. Aoki, Y. Haga, and Y. Onuki, Phys. Rev. Lett. **90**, 077004 (2003).
4. S. Elgazzar, I. Opahle, R. Hayn, and P. M. Oppeneer, Phys. Rev. B: Condens. Matter **69**, 214510 (2004).
5. K. Haule, C.-H. Yee, K. Kim, Phys. Rev. B: Condens. Matter **81**, 195107 (2010).
6. J. A. Hertz, Phys. Rev. B: Solid State **14**, 1165 (1976).
7. A. J. Millis, Phys. Rev. B: Condens. Matter **48**, 7183 (1993).

8. Q. Si, S. Rabello, K. Ingersent, and J. L. Smith, Nature (London) **413**, 804 (2001).
9. P. Gegenwart, Q. Si, and F. Steglich, Nat. Phys. **4**, 186 (2008).
10. H. Shishido, R. Settai, H. Harima, and Y. Õnuki, J. Phys. Soc. Jpn. **74**, 1103 (2005).
11. L. B. Ioffe and A. J. Millis, Phys.—Usp. **41** (6), 595 (1998).
12. T. Park, V. A. Sidorov, F. Ronning, J.-X. Zhu, Y. Tokiwa, H. Lee, E. D. Bauer, R. Movshovich, J. L. Sarrao, and J. D. Thompson, Nature (London) **456**, 366 (2008).
13. M. Yu. Kagan and V. V. Val'kov, JETP **113** (1), 156 (2011).
14. S. Nakatsuji, D. Pines, and Z. Fisk, Phys. Rev. Lett. **92**, 016401 (2004).
15. S. Watanabe and K. Miyake, J. Phys. Soc. Jpn. **79**, 033707 (2010).
16. A. F. Barabanov, K. A. Kikoin, and L. A. Maksimov, Theor. Math. Phys. **20** (3), 881 (1974).
17. V. A. Moskalenko, Theor. Math. Phys. **110** (2), 243 (1997).
18. V. V. Val'kov and D. M. Dzebisashvili, Theor. Math. Phys. **157** (2), 1565 (2008).
19. N. M. Plakida, Theor. Math. Phys. **5** (1), 1047 (1970).
20. V. V. Val'kov and D. M. Dzebisashvili, JETP **110** (2), 301 (2010).
21. Y. Bang, M. J. Graf, A. V. Balatsky, and J. D. Thompson, Phys. Rev. B: Condens. Matter **69**, 014505 (2004).

Translated by R. Tyapaev